INVESTIGATION OF JET-LOOP BIOREACTOR JET AERATOR OPERATION MODES

Vladislav Yaroshevsky[1], Serhii Yasynskyi[1], Tetiana Osypenko[1], Volodymyr Bulgakov[2], Yevhenii Bakulin[2], Dainis Viesturs[3], Valentina Bakulina[2]
[1]Engineering and Technological Institute "Biotekhnika" of NAAS, Ukraine;
[2]National University of Life and Environmental Sciences of Ukraine, Ukraine;
[3]Latvia University of Life Sciences and Technologies, Latvia
adolfs.rucins@lbtu.lv

Abstract. The paper is devoted to the jet aerator operation modes investigation of the jet-loop bioreactor. Loop bioreactors with jet aeration are promising fermentation equipment for submerged microbial cultivation, but the processes of air and fermentation medium jet mixing have been poorly studied yet. Therefore, the jet aerator as the main device of the bioreactor enabling oxygen mass transfer is the research subject. Optical flow visualization method with rheoscopic fluid (stearic acid water suspension) in combination flow parameter direct measurements were used in the study. A jet aerator of the FT-0.325p pilot-scale jet-loop bioreactor for microbial pesticides manufacturing, and a model of its axial cross-section at a scale of 1:1 was used in the research. Flow visualization took place in a flat model of the jet aerator axial cross-section made from a 1.5 mm thick acrylic glass plate. It was indicated that main jet mixing of flows occurred in air-fluid conglomerates, which were a suspension with little air jets. Flow pattern analysis allowed summarizing of air and fluid flow interaction peculiarities at different flow modes in two main flow schemes, existence of which could be evaluated by static pressure ratio in air and fluid inlets p_s. The effective aeration mode occurred at p_s = 0.87…1.18 and is characterised by most of the jet aerator space occupied by air-fluid conglomerates (suspension). The reduction of p_s led to unmixed fluid volume increasing in the aerator and poor aeration conditions. Thus, identification of the jet aeration efficiency could be ensured by static pressure ratio range keeping of air and fluid flows at the aerator inlets. A comparison of flow parameters allowed to confirm reproduction of the flow pattern in the model and jet aerator device. That permitted using effective aeration modes detected for the model by flow visualization in the jet aerator operation. Comprehensive studies of flows in hydraulic equipment with additional optical flow visualisation allow the correlation of changes in the flow pattern with hydrodynamic parameters. This contributes to a deeper understanding of the physical nature of the processes taking place and allows creation of more accurate mathematical models.

Keywords: jet aeration, flow pattern, air-fluid conglomerate, model, flow visualization.

Introduction

Jet-loop reactor (JLR) is a perspective equipment for various applications of fermentation technology [1] including microbial pesticides manufacturing [2]. Due to increased oxygen mass transfer JLR catches attention of many technologists and bioreactor designers [3]. Such equipment development and operation became a topic of recent researches [4].

Direct mixing of the medium and air in a separate device – jet aerator results in aeration efficiency enhancing in comparison with stirred tank bioreactors, which are the widest-spread fermentation equipment [5]. However, aeration efficiency as a rule is evaluated by means of quantitative indicators such as aeration rate [3] or volumetric mass transfer coefficient [5] without reference to air-fluid mixing peculiarities, i.e. qualitative indicators. Therefore, in most cases, aeration efficiency increasing is associated with the air flow rate, realized by power input enhancement of external pumps and/or air compressors. As it was shown in our previous work [6], such approach did not guarantee entire mixing of air and fluid, and in some cases promoted slug flow formation.

The crucial component of JLR is a jet aerator, which is generally an ejector. Its key target is flow jet mixing of fermentation medium (fluid) and air supplied to the jet aerator inlets. There are several types of jet aerator operation regimes [2; 4]. The most of them expecting air suction by fluid flow due to Venturi effect [1; 3; 4]. However, low efficiency of this regime (standard for classical air-fluid ejectors) limits its widespread using in fermentation technology. Another operation regime was proposed for this disadvantage removal [2; 6]. It expects jet mixing of pressured flows of air and fermentation medium, and allows aeration rate regulation in wide range [2]. However, jet mixing of air and fluid is poorly investigated for this regime effective using in practice.

Our previous work dealt with air and fluid interaction peculiarities in a jet aerator studied by optical flow visualization method with rheoscopic fluid [6]. Flow pattern analysis in different parts of the jet aerator model in flow regimes equal to operating enabled qualitive evaluation of the aeration process.

This study is aimed to operation mode identification optimal for jet aeration efficiency based on the analysis of the flow pattern combined with flow parameters.

Materials and methods

The jet aerator (Fig. 1a) of JLR for microbial pesticide manufacturing of 325 dm^3 total volume (FT-0.325p, ETI "Biotekhnika" NAAS) and its axial section model (Fig. 1b) were used in the study. The jet aerator consisted of three main parts: the nozzle, the chamber (T-joint), and the Venturi tube. The nozzle and Venturi tube of the aerator were made of stainless steel, and the chamber was made of brass. The model of jet aerator axial section was made of an acrylic glass plate 1.5 mm thickness in the 1:1 scale.

a) b)

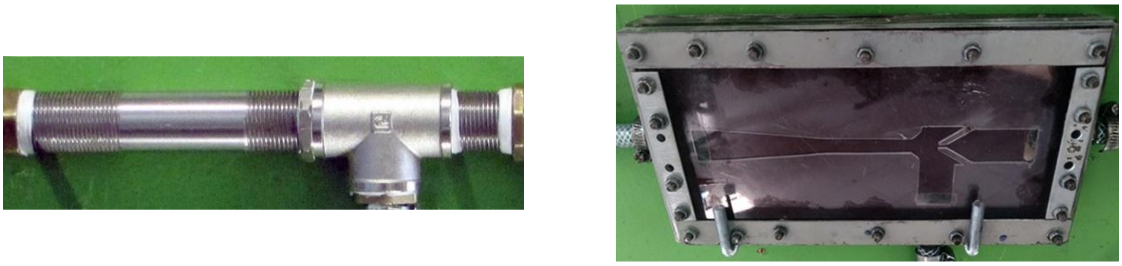

Fig. 1. **Jet aerator (a) and the model of jet aerator axial section (b) installed into test section**

The jet aerator design was equal to a classical ejector (Fig. 2). However, the operation mode differed from the air-fluid ejector's as both air and fluid flows were pressured, and air sprayed through the nozzle into fluid flow. The jet aerator length was 214 mm. The inner diameters of air, fluid, and mixture ducts were 20 mm. The nozzle and Venturi tube diameters were 3 mm and 10 mm respectively.

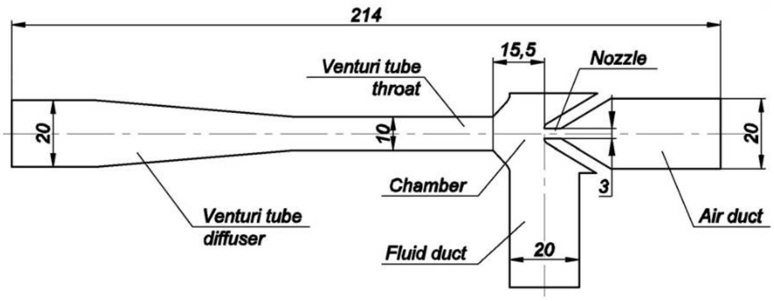

Fig. 2. **Design of jet aerator (dimensions in mm)**

The experiments were made on the same facility (Fig. 3) as in our previous work [6]. It contained the vortex pump (Koer KP.P15-GRS 10) and air compressor (Resun ACO-012) used in the loop of JLR. Fluid and air flow rates were determined by a fluid flowmeter (Kobold DSV-1104H.00.R15) and air flowmeter (Metrix) respectively. Fluid accumulated in the 10 dm^3 tank and was supplied to the test section through a needle valve for flow rate regulation. The air was supplied to the test section through a 10 dm^3 air receiver tank for pressure pulsation damping.

The test section 1a was used in the flow visualization experiments. It consisted of two covering acrylic glass plates and the model fixed between them. The back plate contained flow channels for rheoscopic fluid and air supply of the model and the air-fluid mixture drained from it. A non-transparent epoxide paper plate (getinaks) was encased between the back covering plate and the model. LED strip was used for the test section illumination. Flow pattern was detected by a digital camera (Canon PowerShot SX412 IS) in the jet aerator model.

The hydraulic experiments were made on test section 1b. It contained the jet aerator device and connection fittings.

The same rheoscopic fluid was used in experiments with the jet aerator model and device for enabling comparison of the results. It was a water suspension of stearic acid (1:20 by mass), which had good optical properties for flow visualization and neglectable deviation of viscosity from water [6; 8]. The rheoscopic fluid was made by standard technique [8]. Its properties at 24 °C were: the density – 0.972 g·cm^{-3}, the kinematic viscosity coefficient – 0.926·10^{-6} m^2·s^{-1}.

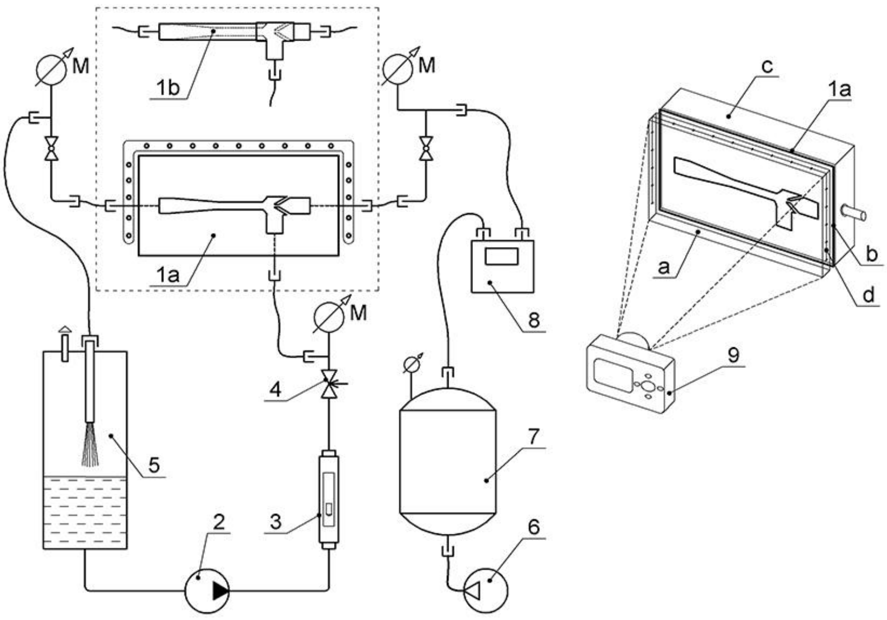

Fig. 3. **Experimental facility:** 1a – test section with jet aerator model; 1b – test section with jet aerator device; 2 – pump; 3 – fluid flowmeter; 4 – needle valve; 5 – fluid tank; 6 – air compressor; 7 – air receiver tank; 8 – air flowmeter; 9 – digital camera; M – pressure gauge. The structure of test section 1a: a – front covering plate; b – model; c – back covering plate with flow channels; d – LED strip

The experimentation procedure was in general the same for flow visualization and hydraulic experiments. Rheoscopic fluid and pressured air were supplied to the test section by a pump and air compressor respectively. The jet aerator operation modes were changed by fluid flow rate (Q_f) regulation by the needle valve in the range (2…6) $dm^3 \cdot min^{-1}$ with a step of 1 $dm^3 \cdot min^{-1}$. The indications of flow meters and the pressure gauge were detected by two digital cameras at the same time for obtaining transient values of flow rates and pressures. Additionally, in flow visualization experiments jet mixing of air and rheoscopic fluid flows was caught on video on each value of fluid flow rate. All experiment series were made in triple.

The data analysis was made by video recordings of flow meters and pressure gauges studied in Vegas Pro. 20.0 software and further processing in MS Excel. Flow parameter statistical analysis was also made in MS Excel by standard technique [9]. Arithmetic means of pressures and flow rates, and standard deviations were found. Relative and absolute measurement errors were calculated for 95% confidence.

The dynamics of the flow pattern was analysed at images obtained from video records by a frame-by-frame method. Flow pattern geometry was determined by dimensioning in AutoCAD 2024 software environment.

Dimensionless flow rate q and dimensionless static pressure p_s were determined for additional indication of the jet aerator operation modes. They were calculated as a ratio of volumetric flow rates of fluid and air for q, and a ratio of static pressures of air and fluid for p_s [4; 6; 7]:

$$q = \frac{Q_f}{Q_a}, \tag{1}$$

$$p_s = \frac{P_{st\,a}}{P_{st\,f}}, \tag{2}$$

where q – dimensionless flow rate;
p_s – dimensionless static pressure;
Q_f, Q_a – volumetric flow rates of fluid and air respectively, $dm^3 \cdot min^{-1}$;
$P_{st\,a}$, $P_{st\,f}$ – static pressures of air and fluid respectively at the jet aerator inlets, kPa.

Results and discussion

Aeration efficiency in JLR depends largely on peculiarities of air and fermentation medium flows interaction in the jet aerator, as the main aeration process takes place exactly in this device. Therefore, these peculiarities understanding is very important for microbial growth in the bioreactor. Optical flow visualization method is a powerful tool for their detection and investigation [6; 8; 10].

In our previous work we defined that air and rheoscopic fluid flows did not mix in the aerator chamber and moved in parallel [6]. Jet mixing began in the Venturi throat and developed through the diffuser. Interaction of flows in the Venturi throat edge was crucial for jet mixing and strongly depended on the space occupied by each flow in this cross-section.

Aeration efficiency as a rule is determined by the oxygen transfer rate [3; 11]. It depends on the volumetric oxygen mass transfer coefficient $k_L\alpha$, which cannot be obtained by direct measurements. It is the product of the mass transfer coefficient k_L and the interfacial area per fermentation medium volume α [3]. Interfacial area increasing is one of the standard ways for aeration efficiency enhancing. In our case, it means that jet aerator operation mode with contribution to α increasing is more efficient in comparison with all others. Furthermore, there is a correlation of interfacial area and flow pattern of air and fluid medium flows interaction in various types of bioreactors [4]. Such interaction takes place in the jet aerator as we reported earlier [6]. Thus, jet aeration efficiency of different modes could be compared by the flow pattern of air and fluid flow interaction obtained by flow visualization methods.

The detailed flow pattern analysis was made for operation modes in the jet aerator model (Fig. 4). There were obtained some new peculiarities of air and rheoscopic fluid interaction. First of all, it was indicated that air-fluid conglomerates in the Venturi tube are in fact air-fluid suspension (but not the fluid) with small air jets. Therefore, the interfacial area α and the corresponding $k_L\alpha$ value in such flow pattern should be much bigger comparing to fluid flow bordering with air caverns. Thus, air-fluid conglomerate was taken as optimum flow pattern for aeration efficiency in the jet aerator.

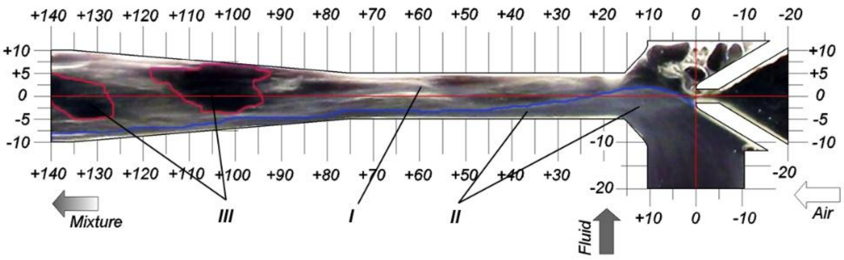

Fig. 4. **Flow pattern in jet aerator model** (the scale in mm): I – air-fluid conglomerate; II – unmixed fluid flow; III – unmixed air (cavern)

The analyses of flow pattern changing in different operation modes allowed summarising all operation modes in only two jet mixing flow schemes (Fig. 5).

The first flow scheme (Fig. 5a) took place at the fluid flow rate $Q_f \leq 4.5$ dm^3·min^{-1} and is characterised by increased air flow rate $Q_a = 3…14$ dm^3·min^{-1}. It contained air-fluid conglomerates (mixture), unmixed fluid flow near the wall, and unmixed air volumes (caverns) in the Ventri tube. The presence of the last ones indicated batch-type air fluid mixing when fluid batch saturated by air and became the suspension (the conglomerate). Air-fluid conglomerates and unmixed air volumes alternated in the Ventri tube. Air caverns travelled downstream the Ventri tube reacting with unmixed fluid flow by disturbance of the border layer. That initiated additional mixing. Thus, aerator operation modes matching such flow scheme could be considered as effective for aeration.

The second one (Fig 5. b) took place at the fluid flow rate $Q_f > 4.5$ dm^3·min^{-1}. It is characterized by the reduction of the air flow rate up to $Q_a = 1$ dm^3·min^{-1}. However, air caverns became three times smaller and formed rarely. Air-fluid conglomerates (the optimum flow pattern for efficient jet aeration) occupied smaller Venturi tube volume because the unmixed fluid flow volume increased. Thus, operation modes matching the flow scheme could be considered as ineffective for aeration.

The analysis showed that mixing of fluid and air flows strongly depended on initial interaction of unmixed jets in the camber. The unmixed air flow throttled by unmixed fluid flow and that resulted in the air flow rate reduction against the fluid flow rate increasing. This process could be observed on both flow schemes (Fig. 5) by movement of boundary between air and fluid flows (blue line) in the chamber. Therefore, static pressure of each flow as one of the flow shape-determining parameters must be crucial for jet initial interaction, and static pressure ratio should correlate with the flow boundary movement.

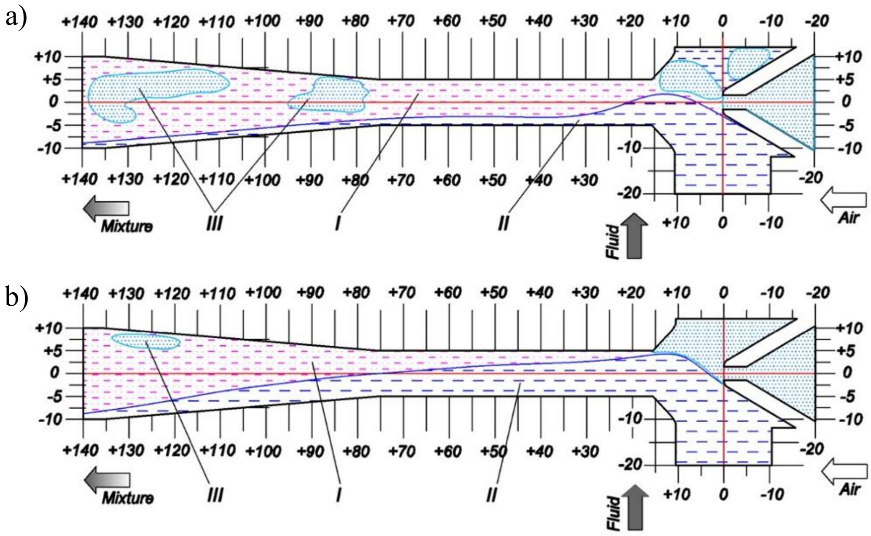

Fig. 5. **Flow schemes in the jet aerator model at different operation modes** (the scale in mm): a – flow scheme for $Q_f < 4.5$ dm^3·min^{-1} ($0.87 < p_s < 1.18$), b – flow scheme for $Q_f \geq 4.5$ dm^3·min^{-1} ($0.71 < p_s < 0.82$), I – air-fluid conglomerate, II – unmixed fluid flow, III – unmixed air (cavern)

Thus, the static pressure ratio or dimensionless static pressure p_s could be used as one of the flow scheme existence conditions. Effective aeration flow scheme (Fig. 5 a) existed at p_s = 0.87…1.18. Flows mixing by the second scheme (Fig. 5 b) took place at p_s = 0.71…0.82. Reduction of the dimensionless static pressure was accompanied by boundary displacement in the direction perpendicular to the air inlet (Fig. 5).

We suppose that repetition of p_s in the jet aerator model and jet aerator device should be one of the main conditions of flow scheme repetition. It stands to mention that the flow pattern in a flat model and the modeled device axial section repetition is ensured by static pressure correspondence in the inlets in optical flow visualization [12]. On the other hand, the model and the jet aerator were tested in the conditions equal to this device operation in bioreactor loop. The air compressor and circulation pump of the bioreactor FT-0.315p were used in experimental facility.

Experimental curves $p_s = f(q)$ for the jet aerator and its model obtained by three test series averaging are shown in Fig. 6. One can see that both curves have an equal shape, which indicates compatibility of hydrodynamic processes (flow pattern) in the model and device. Jet aerator's curve lays at the p_s = 0.85…1.18 (dotted lines), i.e. the device operated at the efficient aeration zone.

The dependence $P_{st} = f(Q)$ analysis for air and rheoscopic fluid flows (Fig. 7) gives additional evidence of flow mixing repentance in the jet aerator model and device. Fluid flow and air flow curves have equal shapes, which indicate that flow parameters are changed at equal dependences. Consequently, mixing of flows occurred at the same flow schemes. The curve slight deflection for the model and device is caused by differences in quasi two-dimensional flows in the model and three-dimensional flows in the jet aerator. Flow developing in the third dimension of the jet aerator predictably dislocated the curves in the direction of the flow rate increasing.

The flow parameter comparison for the jet aerator model and device indirectly confirmed Bychkov's suggestion [12] about dependence of the flow pattern reproducibility in a flat model and the modelled device axial section from static pressure correspondence in the inlets.

The study showed that air flow rate increasing led to incomplete mixing of air into fluid flow with air cavern forming in the mixture (Fig. 4, 5a). Therefore, part of the air volume was not used effectively. This fact could not be accounted at a diagram like $p_s = f(q)$, which indicated aeration rate (corelated with q) with pressure ratio on inlets of the aerator. Efficient and inefficient jet aerator operation modes cannot be matched with the flow parameters as pressures or flow rates only (Fig. 6, 7). They require flow pattern analysis. The study results showed that efficiency for the aeration jet device operating mode could be described as p_s range, maintenance of which ensured formation of a stable flow pattern in the aerator efficient for air and fluid jet mixing, i.e. for obtaining air-fluid suspension.

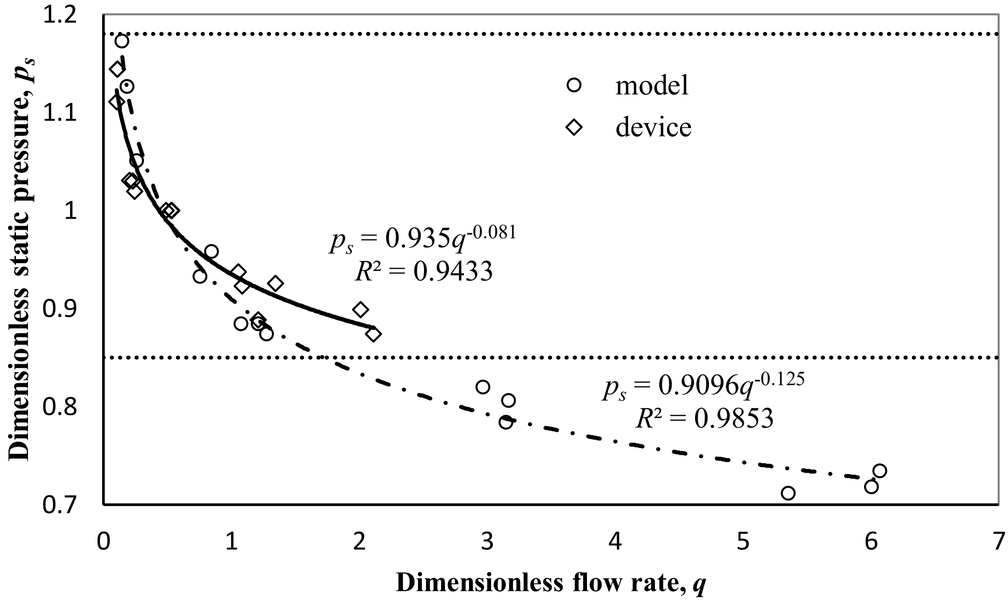

Fig. 6. **Experimental curves $p_s = f(q)$ for the jet aerator model and device**

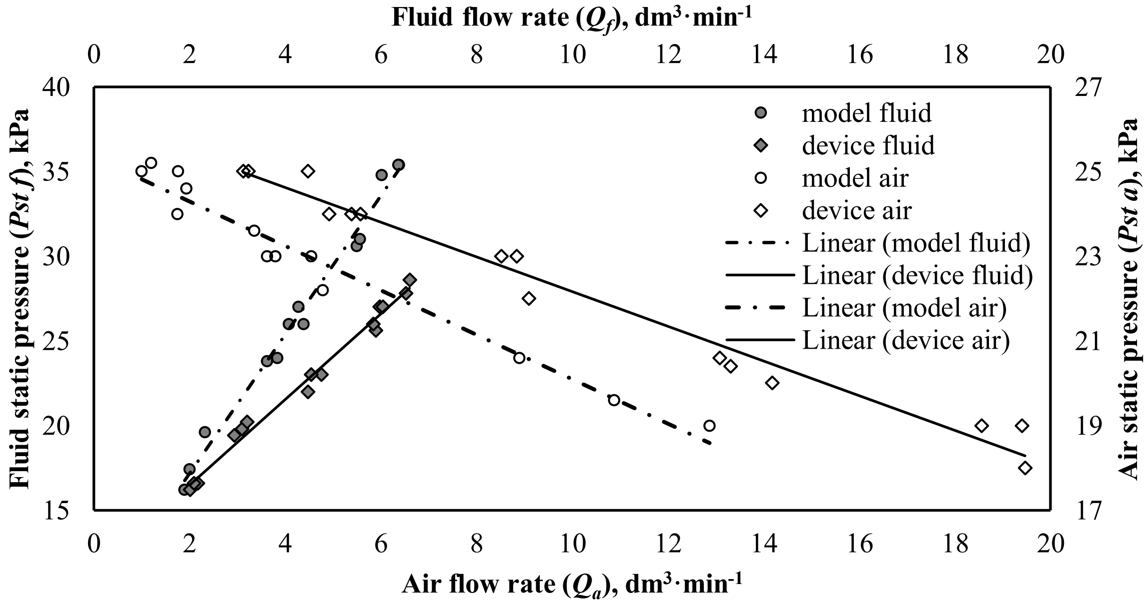

Fig. 7. **Experimental curves $P_{st} = f(Q)$ for the jet aerator model and device**

The studies of jet aeration in JLR as a rule connect the mass transfer coefficient $k_L\alpha$ enhancement with increasing of the interfacial area between air and fluid media flows α [3-5]. It is considered that interfacial area is increasing proportionally to aeration rate increasing [11], which is not exactly so due to jet mixing peculiarities described above.

Standard correlations for $k_L\alpha$ in JLR include power consumption to fluid media volume ratio and superficial air velocity [1; 4; 5]. In fact, such correlations should reflect energy distribution of air flow in a fluid volume, i.e. jet mixing flow pattern. However, computing methods for power consumption based on multiplication of fluid flow rate and static pressure difference in the ejector [4; 11] could not account for the flow pattern effect on mixing.

Thus, aeration efficiency evaluated by $k_L\alpha$ based on correlations with fluid and air flow parameters does not consider qualitative assessment of jet mixing. Flow visualization methods in our opinion can be the ground of more complex correlations for the mass transfer coefficient evaluation matching to the flow pattern and flow parameter both.

Conclusions

1. Flow pattern for air and fluid mixing in a jet aerator in different operation modes could be summarized by flow schemes inside, which structure of flow interaction is kept essentially without changes.
2. The aerator operation mode (flow scheme) effectiveness could be evaluated by the aerator space occupied by air-fluid conglomerates, which are air-fluid suspension with small air jets, i.e. the flow pattern optimum for jet mixing. Static pressure ratio of air and fluid p_s could be considered as a flow scheme existence condition. Effective flow mode for the described jet aerator geometry existed at p_s = 0.87…1.18. The reduction of p_s was accompanied by boundary displacement between air-fluid conglomerates and unmixed fluid with the volume increasing of the last one.
3. Flow pattern repetition in a jet aerator axial section model and device could be ensured by static pressure correspondence in the inlets of air and fluid in optical flow visualization. However, additional correlations considering third dimension action on the flow pattern in the device is required.
4. Jet aeration impartially is classified as an effective aeration technique, which ensured obtaining air-fluid suspension in JLR loop. The efficiency of aeration is determined by the flow pattern of air and fluid mixing in the aerator. Such flow pattern analysis could be done by different flow visualization techniques. However, its absence could affect on data evaluation accuracy including the rate of the oxygen mass transfer coefficient. Therefore, correlations determining $k_L\alpha$ with account of the flow pattern of mixing is a very crucial task.

Author contributions:

Conceptualization, V.Y. and V.B.; methodology, V.Y. and T.O.; software, S.Y.; validation, V.B.; formal analysis, T.O., A.R. and V.B.; investigation, V.Y., S.Y. and T.O.; data curation, V.B.; writing – original draft preparation, V.Y., D.V., Y.B. and V.B.; writing – review and editing, V.B.; visualization, V.Y., Va.B.; project administration, V.B. All authors have read and agreed to the published version of the manuscript.

References

[1] Warmeling H., Behr A., Vorholt A. Jet loop reactors as a versatile reactor set up – Intensifying catalytic reactions: A review. Chemical Engineering Science, vol. 149, 2016, pp. 229-248. DOI: 10.1016/j.ces.2016.04.032
[2] Yaroshevsky V., Krutyakova V., Belchenko V., Ivanovs S., Bulgakov V. Development and research of new media jet aeration scheme in a loop bioreactor producing microbiological products. Acta Technologica Agriculturae. vol. 24, 2021, pp. 124-128. DOI: 10.2478/ata-2021-0021
[3] Ughetti M., Jussen D., Riedlberger P. The ejector loop reactor: Application for microbial fermentation and comparison with a stirred-tank bioreactor. Engineering in Life Science, vol. 18(5), 2018, pp. 281-286. DOI: 10.1002/elsc.201700141
[4] Moresi M. Design and operation of a multifunctional pilot-scale bioreactor for enhanced aerobic fermentation. Fermentation, vol. 11(2), 2025, p. 101. DOI: 10.3390/fermentation11020101
[5] Weber S., Schaepe S., Freyer S., Kopf M.-H., Dietzsch C., Effect of ejector operation on the oxygen transfer in a pilot jet loop reactor. Chemical Engineering & Processing: Process Intensification. vol. 131, 2018, pp. 43-50 DOI: 10.1016/j.cep.2018.07.007
[6] Yaroshevsky V., Yasynskyi S., Bulgakov V., Ruzhylo M., Aboltins A., Rucins A., Polishchuk D. Jet aeration study by flow visualization method with rheoscopic fluid. Proceedings of International conference "Engineering for rural development", May 21-23, 2025, Jelgava, Latvia, pp. 116-122. DOI: 10.22616/ERDev.2025.24.TF023
[7] Zhao J., Wei X., Zou J., Zhang Y., Sun J., Liu Z. Research on performance optimization of gas–liquid ejector in multiphase mixed transportation device. Journal of Mechanics, vol. 38, 2022, pp. 22-31. DOI: 10.1093/jom/ufac001

[8] Borrero-Echeverry D., Crowley C.J., Riddick T.P. Rheoscopic fluids in a post-Kalliroscope world Physics of Fluids. vol. 30, 2018, 087103. DOI: 10.1063/1.5045053
[9] Divisi D., Di Leonardo G., Zaccagna G., Crisci R. Basic statistics with Microsoft Excel. Journal of Thoracic Disease, vol. 9(6), 2017, pp. 1734–1740. DOI: 10.21037/jtd.2017.05.81
[10] Muller K, Greidanus AJ, Dash A, Poelma C. Bullet time Taylor-Couette: Unwrapping the 360-degree field of view for rheoscopic flow visualization. In 20th International Symposium on Applications of Laser and Imaging Techniques to Fluid Mechanics, July 11-14, 2022, Lisbon, Portugal. https://research.tudelft.nl/files/149080975/120_paper.pdf
[11] Weber S., Schaepe S., Kopf M.-H, Freyer S., Dietzsch C. Jet aeration as alternative to overcome mass transfer limitation of stirred bioreactors. Chemie Ingenieur Technik, vol. 90, 2018, pp. 1250-1250. DOI: 10.1002/cite.201855260
[12] Бычков Ю.М. Визуализация тонких потоков несжимаемой жидкости (The visualization of thin incompressible fluid flows), Кишинев: Штиинца, 1980. 132 p.